The partitioning of energy amongst vibration, rotation, and translation during the dissociation of *p*-difluorobenzene–Ar neutral and cation complexes

Susan M. Bellm and Warren D. Lawrance[a)]
School of Chemistry, Physics and Earth Sciences, Flinders University, GPO Box 2100, Adelaide, South Australia 5001, Australia

(Received 28 October 2002; accepted 14 November 2002)

The dissociation dynamics of *p*-difluorobenzene–Ar and *p*-difluorobenzene–Ar^+ have been investigated from the $\overline{5^1}$ level in S_1 and the $\underline{29_2}$ level in D_0, respectively. The technique of velocity map imaging has been used to determine the translational energy release distributions. In the case of $\overline{5^1}$ *p*-difluorobenzene–Ar, dispersed fluorescence spectra provide the distribution of vibrational energy in the *p*-difluorobenzene fragment. A significant fraction of the *p*-difluorobenzene products are formed in the 0^0 level. From the translational energy release data the rotational energy distribution within 0^0 can be inferred. The results show that the average rotational energy is 380 cm^{-1}, >5 times the average translational energy of 70 cm^{-1}. This rotational excitation infers that dissociation occurs with the Ar atom significantly displaced from its equilibrium position above the center of the aromatic ring. From the average rotational energy it is determined that the Ar atom is, on average, displaced by 1.8–3.7 Å from the center of the aromatic ring at dissociation, i.e., the Ar atom is beyond the carbon atoms. In the case of dissociation from the $\underline{29_2}$ level of *p*-difluorobenzene–Ar^+, the vibrational distribution within the *p*-difluorobenzene$^+$ product is not known, however it can be inferred from previous studies of dissociation within S_1. As for the $\overline{5^1}$ *p*-difluorobenzene–Ar case, the evidence suggests that dissociation leads to significant rotational excitation of *p*-difluorobenzene$^+$. There are a limited number of destination vibrations within the *p*-difluorobenzene and *p*-difluorobenzene$^+$ fragments for dissociation from $\overline{5^1}$ (S_1) and $\underline{29_2}$ (D_0), respectively. Hence there are only a few, widely separated, values for the combined translational and rotational energy available. Despite this, the translational energy release distributions in both cases are smooth and structureless. In the limit of no rotational excitation of the polyatomic fragment, the translational energy release distributions would show peaks only at energies corresponding to populated vibrational states of the product. The absence of such peaks indicates that rotational excitation of the product occurs for all vibrational states, reducing the average translational energy released and smearing the distribution. © *2003 American Institute of Physics.*
[DOI: 10.1063/1.1535419]

I. INTRODUCTION

Aromatic–rare gas, –diatomic, and –small polyatomic van der Waals complexes have been examined extensively over the past two decades. Because of favorable spectroscopic and photophysical properties, studies of vibrational predissociation (VP) have focused on behavior within the first excited singlet state of these complexes. VP is now known to generally occur via a sequential mechanism involving an intramolecular vibrational energy redistribution (IVR) from the initially excited vibration within the aromatic chromophore to van der Waals modes, followed by dissociation.[1] At low initial vibrational energies, and correspondingly low vibrational state densities, the IVR rate is often mode specific and this is responsible for the VP rate itself being mode specific.

Using dispersed fluorescence, the vibrational states in the aromatic fragment populated during VP have been identified in a number of cases. Most relevant to the present work are the studies of *p*-difluorobenzene complexes by Parmenter's group.[2–4] Recently, mass analyzed threshold ionization (MATI) has been shown to provide an alternative method for observing the nascent vibrational population.[5,6] There were early hopes that VP of van der Waals complexes would provide an alternative view of vibrational energy transfer during collisions, with predissociation being a ''half collision'' process.[7] However, while VP has proved to be a highly mode specific process, as is collision-induced vibrational energy transfer (VET), the state-to-state branching ratios are often different from those seen for VET. One issue that arises in comparing VP and VET is that van der Waals molecule dissociation is considered to involve a constrained initial geometry.[8]

While there are reasonably extensive data concerning the partitioning of energy into the vibrational states of the aromatic product, there is relatively little known concerning its rotational and translational energy. A feature of the

a)Author to whom correspondence should be addressed. Electronic mail: warren.lawrance@flinders.edu.au

recent MATI studies of vibrational predissociation in fluorobenzene–Ar (Ref. 5) and *p*-difluorobenzene–Ar (pDFB–Ar)[6] is the broad width to the vibrational bands, indicating substantial rotational excitation of the aromatic fragment. Similar observations have been made in other systems, for example *s*-tetrazine–Ar,[9] aniline–Ar,[10] and pyrimidine clusters.[11] An early study of the translational energy released following dissociation of ethylene dimers indicated that only a small amount of the available energy is transferred into translation in this system, also revealing significant rotational excitation of the fragments.[12] There are few studies of the translational energy released during van der Waals molecule dissociation. In addition to the ethylene dimer, studies in the early to mid-1980s examined benzene dimers[13–15] and the benzene dimer cation.[16] Yoder and Barker have recently measured the translational energy released during dissociation of aromatic–monatomic/small polyatomic complexes with significant vibrational energy in the triplet state (2000–8000 cm^{-1}).[17,18] They found that only small amounts of energy (up to a few hundred wavenumbers) appear in translation, indicating that the products had significant energy remaining in the internal degrees of freedom. Our recent experiments on the translational energy released during dissociation of benzene–Ar^+ and benzene–Ar_2^+ came to a similar conclusion.[19]

Studies of the energy partitioning into the vibrational, rotational, and translational degrees of freedom can provide considerably more information on the dissociation dynamics than the study of partitioning into one of these alone. In this article we present the results of an investigation of the dissociation dynamics of pDFB–Ar neutral and cation complexes. Measurements of the translational energy released (TER) during dissociation from $\overline{5^1}$ (S_1 pDFB–Ar) and $\underline{29_2}$ (D_0,pDFB–Ar^+) are reported. (Note: To differentiate the neutral and cation complexes, an upper bar is used to denote states or transitions within the neutral complex while a lower bar denotes either states of the cation complex or transitions from the neutral to the cation complex.) These measurements are undertaken using the technique of velocity map imaging,[20] an enhanced resolution variant of ion imaging.[21] The high resolution provided by velocity map imaging raises the possibility of observing structure in the TER distributions since for van der Waals molecule dissociation occurring at low vibrational energy there are few vibrational levels accessible to the product. In the case of $\overline{5^1}$, our results are combined with previous measurements of the vibrational distribution of the products[2,3,6] to reveal that the majority of the energy released is to rotation of the pDFB fragment. We show that the conservation of angular momentum implies that, although the equilibrium position has the Ar atom centered above the aromatic ring, the Ar atom is on average well off-center at dissociation. Because the product vibrational state distribution has not been measured for $\underline{29_2}$, the situation for this level is less well established. Nevertheless, we show that it is most likely that the dissociation dynamics also involve significant rotational excitation of the pDFB fragment.

The pDFB–Ar complex has been the subject of a large number of experimental investigations using a variety of approaches, including dispersed fluorescence,[2,3,22] resonance-enhanced multiphoton ionization (REMPI),[23] rotationally resolved UV spectroscopy,[24,25] and mass analyzed threshold ionization (MATI) spectroscopy.[6] *Ab initio* calculations have been employed to predict the geometry and dissociation energy of the complex.[26,27] Recently we have reported an experimental determination of the dissociation energy using velocity map imaging to observe the maximum translational energy released in dissociation in the S_1 and D_0 states of the neutral[28] and cation,[29] respectively.

II. EXPERIMENTAL DETAILS

The experimental setup and the method of data analysis are summarized in a previous publication from this group.[19] Briefly, the pDFB–Ar complex is excited to a chosen vibrational level in S_1 using a pulsed, frequency doubled dye laser. Absorption of a second photon of the same frequency leads to ionization. For $\overline{5^1}$, the dissociation process of interest occurs within S_1 and the ionization step involves ionising the pDFB product. (~25% of complexes are ionized and subsequently dissociate—see Sec. III A.) For $\underline{29_2}$, dissociation does not occur within S_1 on the experimental time scale[2–4,23] and the pDFB–Ar complex is ionized. The ionization process leads to the complex being produced in a number of vibrational states whose population distribution can be determined from photoelectron spectra. For pDFB–Ar^+ produced above the dissociation threshold, dissociation occurs rapidly, producing $pDFB^+$ and Ar. In both experiments $pDFB^+$ ions are produced and their translational energy, gained during the dissociation process, is measured using velocity map imaging. Images are recorded as a histogram of ion count versus position. Cation images are calibrated using photoelectron images of pDFB taken with identical voltage settings but with the polarity reversed. Zero kinetic energy (ZEKE) spectra of pDFB[30] are used to calibrate the photoelectron images.

The images result from the expanding three-dimensional (3D) ion distribution being flattened onto two dimensions at the detector. The 3D distribution is recreated from the image using an inverse Abel transform.[31] For the images reported here there is no anisotropy in the two-dimensional distribution, which is consistent with previous measurements of the dissociation lifetimes for the complex, which show them to be long relative to the rotational period.[2–4,23] This allows the experimental distribution to be collapsed to a one-dimensional distribution of intensity versus image radius (a so-called radial plot) and this distribution processed using the inverse Abel transform.[18] The intensities in the transformed distribution are corrected to provide the desired distribution of intensity versus total translational energy released as discussed in Ref. 18.

III. RESULTS

A. Dissociation of pDFB–Ar from $\overline{5^1}$

The TER distribution obtained from the velocity map image for dissociation following excitation of $\overline{5^1}$ is shown in Fig. 1. The points are the experimental data. As the center of the image is contaminated by a peak due to MPI of pDFB in

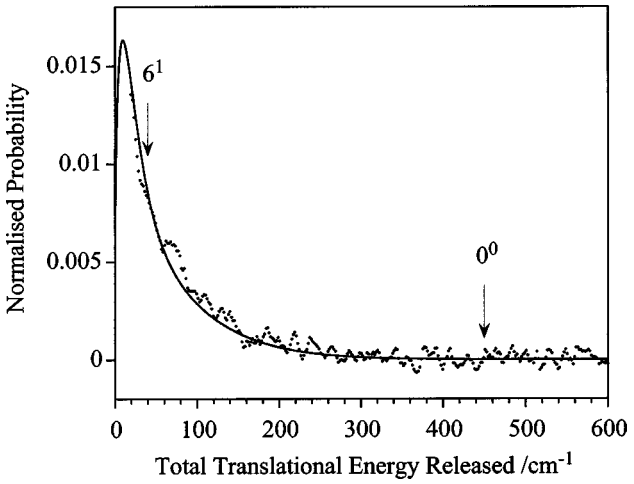

FIG. 1. TER distribution obtained from the velocity map image measured following one color excitation/ionization at the $\overline{5_0^1}$ transition energy of pDFB–Ar. This excitation leads primarily to dissociation from $\overline{5^1}$ in S_1 (see text). Points are the experimental data. The solid line is a fit to the data of the functional form given in Eq. (1). The coefficients from the fit are listed in Table I. The excess energies involved when the 6^1 and 0^0 levels of the pDFB product are populated are indicated by arrows.

the molecular beam, the low translational energy region (<20 cm^{-1}) of the distribution is not observed. However, this region could be observed in our earlier study of benzene–Ar^+ and benzene–Ar_2^+ dissociation, where it was found that the distributions were fit by the form[19]

$$F(E)=\sum_{i=1}^{2} A_i\sqrt{E}\exp(-k_iE). \tag{1}$$

The similarity between the distribution seen here and those seen previously argues that this form is also appropriate here. It is used to fit all distributions obtained. The fit is shown as a solid line in Fig. 1. The parameters describing the fit to the distribution are listed in Table I. Two key features of the distribution are that it is smooth and featureless and that it decays to essentially zero by 300–350 cm^{-1}.

While it is known that complexes excited to $\overline{5^1}$ dissociate [predissociation lifetimes of 2.4 ns (Refs. 2–4) and 4.1 ns (Ref. 23) have been reported], some complexes will be ionized before they have dissociated in S_1. It is thus necessary to determine both the extent to which the TER distribution shown in Fig. 1 pertains to dissociation in S_1 and the consequences of any contribution from dissociation in D_0. $pDFB^+$ and Ar fragments may potentially be produced from pDFB–Ar via either dissociation in S_1 followed by absorption/ionization of the S_1 pDFB fragment or by fragmentation in D_0 after absorption of two photons. Since the energy of $\overline{5^1}$ is above the S_1 dissociation energy and the combined energy of two photons at the wavelength of the $\overline{5_0^1}$ transition is above the D_0 dissociation energy (D_0^+), an image obtained after exciting the $\overline{5_0^1}$ transition may consist of $pDFB^+$ ions produced by both pathways.[28,29]

TABLE I. Values of the constants obtained from fits to the experimental TER distributions using the functional form given in Eq. (1).

Transition	A_1	k_1	A_2	k_2
$\overline{5_0^1}$	7.17×10^{-3}	6.46×10^{-2}	1.68×10^{-3}	1.81×10^{-2}
$\overline{0_0^0}+38\,445$ cm^{-1}	1.70×10^{-3}	3.44×10^{-2}	1.38×10^{-3}	1.36×10^{-2}
$\overline{29_0^2}$	1.27×10^{-3}	8.16×10^{-2}	3.99×10^{-3}	2.40×10^{-2}

The extent of dissociation in S_1 relative to D_0 can be determined from a combination of the photoelectron spectrum and the ratio of pDFB–Ar^+ to $pDFB^+$ ions produced. The photoelectron spectrum reveals the relative vibrational state populations produced in the pDFB–Ar^+ cation by 1+1 REMPI via $\overline{5_0^1}$. From this and a knowledge of D_0^+, the fraction of pDFB–Ar^+ cations produced above D_0^+, and hence dissociate, can be established. (It is known that dissociation occurs sufficiently rapidly above dissociation in D_0 pDFB–Ar that no complex signal is observed in the time of flight mass spectrometer.[6]) The ratio of pDFB–Ar^+ to $pDFB^+$ ions detected shows the amount of undissociated cation to the amount of dissociated pDFB–Ar arising from dissociation in both D_0 and S_1. From the ratio of pDFB–Ar^+ to $pDFB^+$ arising from dissociation in D_0 established from the photoelectron spectrum, the contribution to the $pDFB^+$ signal from dissociation in the S_1 state can be determined.

Unfortunately, due to the low concentration of pDFB–Ar complexes in the expansion relative to bare pDFB, photoelectron images of the complex have a large background. The problem arises because all photoelectrons are detected simultaneously, irrespective of the source, as discussed previously.[19] A good quality spectrum is required for our purpose and we therefore use the corresponding photoelectron spectrum of pDFB obtained after exciting 5_0^1. The photoelectron spectrum is obtained from a photoelectron image and, with the following caveat, matches that reported previously by Sekreta *et al.*[32] The time of flight method employed by Sekreta *et al.* does not provide accurate intensities at low kinetic energy due to loss of electrons through stray electric fields, etc.[33] The use of the ion imaging apparatus enables the population of the low kinetic energy electrons to be accurately determined.[19]

The photoelectron spectrum extracted from the photoelectron image produced by 1+1 REMPI via 5_0^1 is presented in Fig. 2. Two photons at the wavelength of the 5_0^1 transition provide 1441 cm^{-1} in excess of the pDFB ionization potential. Taking into account the reduced ionization potential (237 cm^{-1})[6] and the reduced wavelength of the $\overline{5_0^1}$ transition in pDFB–Ar,[2,3,23] the excess energy of the complex after exciting $\overline{5_0^1}$ will be 1618 cm^{-1}. The ZEKE photoelectron spectrum of the pDFB–Ar complex indicates that there are only a few vibrational levels between 1441 and 1618 cm^{-1} that can be populated and that the population of these will be minimal relative to the lower levels.[31] The pDFB–Ar^+ vibrational state distribution determined from the pDFB 5_0^1 photoelectron spectrum should therefore accurately reflect the distribution produced by two photon ionization of the complex via $\overline{5_0^1}$.

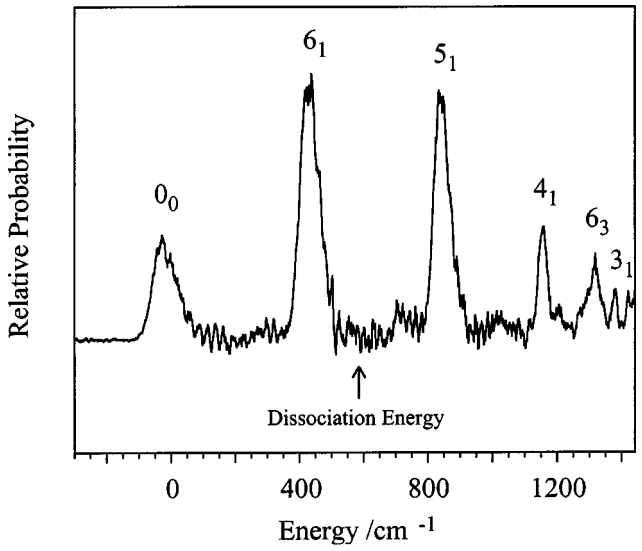

FIG. 2. The photoelectron spectrum following 1+1 REMPI via the 5_0^1 transition of pDFB.

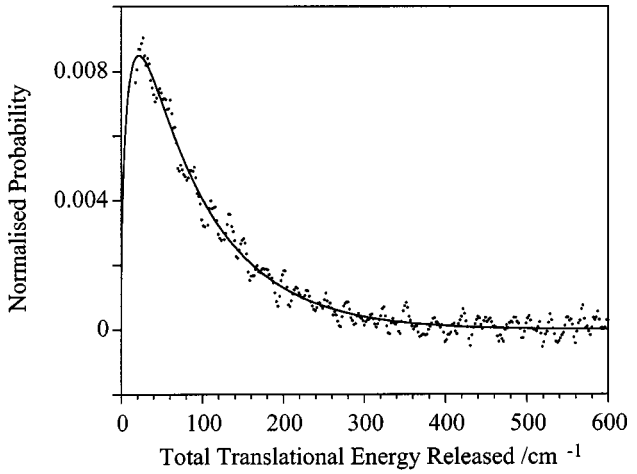

FIG. 3. TER distribution for dissociation of pDFB–Ar^+ within the D_0 state. pDFB–Ar^+ is produced in a $1+1'$ REMPI excitation via the $\overline{0^0}$ level to prevent dissociation occurring in S_1. pDFB–Ar^+ is produced in a number of vibrational states. The energy of the second photon produces pDFB–Ar^+ with the same excess energy produced in the $\overline{5_0^1}$ one color 1+1 REMPI process. Points are the experimental data. The solid line is a fit to the data of the functional form given in Eq. (1). The coefficients from the fit are listed in Table I.

The percentage of cations in each of the D_0 vibrational levels, calculated by integrating the corresponding peaks in the photoelectron spectrum, is shown in Table II. The binding energy of the pDFB–Ar^+ complex is 573 cm^{-1}.[28,29] Ions produced in $\overline{0_0}$ and $\overline{6_1}$, from which dissociation cannot occur, account for 54% of the population. Hence the ratio of pDFB–Ar^+ to $pDFB^+$ from dissociation in D_0 is 54:46, i.e., from this mechanism the signal at the pDFB–Ar mass would be ~1.2 times greater than the signal at the pDFB mass.

pDFB–Ar^+ to $pDFB^+$ ratios were obtained by measuring the ion signal at the pDFB–Ar and pDFB masses using the ion imaging apparatus. Since the detector can only be gated on once per laser shot, these populations could not be monitored simultaneously. The laser was scanned over the $\overline{5_0^1}$ peak while monitoring a single mass. The area of the peak at each mass was calculated and hence the ratio of pDFB–Ar^+ to $pDFB^+$ determined. This was performed a number of times and the measurements averaged. The magnitude of the signal at the pDFB–Ar mass is 0.22 ± 0.09 of the signal at the pDFB mass. It was established above that 46% of the complexes excited to D_0 dissociate. From the observed $pDFB^+$ to pDFB–Ar^+ ratio, we determine that 74%±9% of pDFB–Ar molecules excited via $\overline{5_0^1}$ dissociate in S_1. The remaining ~26% are from dissociation in the D_0 state. Consequently, an image obtained following excitation of the $\overline{5_0^1}$ transition will have a $\sim\frac{3}{4}$ contribution from dissociation in the S_1 state. Nevertheless, the $\sim\frac{1}{4}$ contribution from dissociation in D_0 could be significant, especially if the distributions in S_1 and D_0 are substantially different, and needs to be accounted for.

TABLE II. The relative population of the vibrational levels populated in the 1+1 REMPI photoelectron spectrum of pDFB via the $\overline{5_0^1}$ transition.

Vibrational level	Energy Above D_0^+ (cm^{-1})	Relative population
$\overline{0_0}$	···	18%
$\overline{6_1}$	···	36%
$\overline{5_1}$	264	29%
$\overline{4_1}$	575	8%
$\overline{6_3}$	745	7%
$\overline{3_1}$	802	2%

To explore this issue we have measured the TER distribution for dissociation in D_0 from a distribution of vibrational levels similar to that produced in 1+1 REMPI excitation via $\overline{5_0^1}$. In this experiment pDFB–Ar^+ is produced by two color, $1+1'$ REMPI, the first absorption being via the $\overline{0_0^0}$ transition, which prevents dissociation occurring within S_1. Moreover, absorption of two photons at this frequency produces pDFB–Ar^+ ions in the $\overline{0_0}$ level of D_0 from which dissociation cannot occur. The second photon frequency is chosen to (i) be off-resonance with any pDFB-Ar $S_1 \leftarrow S_0$ transitions and (ii) to access the same set of states in D_0 with a similar population distribution to that produced in the 1 color REMPI excitation via $\overline{5_0^1}$. The TER distributions produced are therefore due to dissociation in D_0 alone. The energy of the second photon produces pDFB–Ar^+ with the same excess energy produced in the $\overline{5_0^1}$ one color 1+1 REMPI process. ν_5 is a Franck–Condon active a_g mode and the population distributions produced in the cation via the $\overline{5_0^1}$ 1+1 REMPI process and the $1+1'$ REMPI via $\overline{0_0^0}$ are similar.[31,32]

The TER distribution arising from dissociation in D_0 alone is shown in Fig. 3. This distribution is fitted to the functional form given in Eq. (1). The fitting parameters are given in Table I. Having determined both the shape of the D_0 TER distribution and the magnitude of its contribution, its influence can be quantitatively accounted for in the analysis.

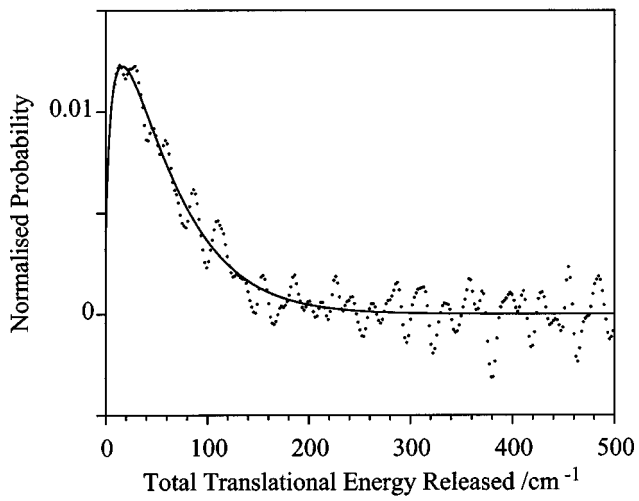

FIG. 4. TER distribution for dissociation following REMPI excitation via the $\overline{29_0^2}$ transition. This excitation leads predominantly to dissociation from the $\underline{29_2}$ level in the D_0 state of the cation (see text). Points are the experimental data. The solid line is a fit to the data of the functional form given in Eq. (1). The coefficients from the fit are listed in Table I.

B. Dissociation of pDFB–Ar$^+$ from $\underline{29_2}$

To study dissociation occurring from a specific level within the cation complex we chose to pump the $\overline{29_0^2}$ transition and ionize in a one color 1+1 REMPI process. Despite $\overline{29^2}$ being above the dissociation threshold in S_1, the $\overline{29_0^2}$ transition was chosen because (i) dissociation from $\overline{29^2}$ is known to be very slow and is uncompetitive with the ionization step,[3,23] and (ii) the Franck–Condon factors for ionization from $\overline{29^2}$ lead to $\underline{29_2}$ being essentially the only state above dissociation populated in D_0, as shown through the photoelectron spectrum.[32]

The TER distribution obtained after exciting the $\overline{29_0^2}$ transition is shown in Fig. 4. The fit to the functional form in Eq. (1) is shown as a solid line in this figure. The fitting parameters are given in Table I. The distribution has the same shape as those presented earlier, peaking at very low translational energy and then showing an exponential-like fall to around zero by $\sim$300 cm^{-1}.

The issue to be determined in the first instance is what states are contributing to the TER distribution seen in Fig. 4. It is readily shown that dissociation within S_1 is a quite minor contributor at best. First, the rate constants determined by O *et al.*[3] and by Jacobson *et al.*[23] both show that dissociation from $\overline{29^2}$ is significantly slower than from other levels (a factor of $\sim$10 slower than dissociation from $\overline{5^1}$, for example). τ_{VP} is 18 ns (Ref. 3) or greater,[23] which means that dissociation within S_1 will not compete with ionization of the complex. Second, the state-to-state dissociation rate constants show that from $\overline{29^2}$ 53% of complexes dissociate to 6^1 [E_{trans}(max)=103 cm^{-1}], 36% to 29^1 [E_{trans}(max) =73 cm^{-1}] and 11% to 0^0 [E_{trans}(max)=513 cm^{-1}].[3] Thus only 11% of the S_1 dissociation products will have a translational energy greater than 103 cm^{-1}. Clearly the distribution in Fig. 4 has much more than 11% in excess of 103 cm^{-1}. Moreover, there is no evidence for a discontinuity at 103 cm^{-1} as one would expect from $\overline{29^2}$ given the vibrational state distribution of the fragments. The evidence therefore supports the proposition that the translational energy distribution obtained following excitation of $\overline{29_0^2}$ is overwhelmingly due to dissociation from $\underline{29_2}$ in D_0.

IV. DISCUSSION

Because there are different issues in relation to dissociation from $\overline{5^1}$ versus $\underline{29_2}$, we discuss each separately. The common features are summarized in Sec. V.

A. Dissociation of pDFB–Ar from $\overline{5^1}$

The first issue to examine is the distribution of population amongst the vibrational levels of the pDFB product. This was first reported by Parmenter and co-workers using dispersed fluorescence spectroscopy.[2–4] They assigned the nascent population to the 6^1 (51%) and 0^0 (49%) levels. 6^1 and 30^1 cannot be distinguished in dispersed fluorescence and the authors assigned the population to 6^1 on the basis that the vibrational changes generally found for vibrational predissociation in pDFB–Ar suggest 6^1 to be a more important channel than 30^1. Using MATI spectroscopy, Lembach and Brutschy have also determined the monomer states that are populated.[6] Like Parmenter, they find that the 0^0 and 6^1 levels are populated following dissociation in S_1. However, they report that the intensity of some vibrational predissociation bands in the MATI spectrum cannot be accounted for if dissociation proceeds such that only 6^1 and 0^0 are populated. They deduced that some population could also be produced in either one or a combination of 17^1, 27^1, 30^1, 30^2 and 30^3 and suggested that, possibly due to the resolution of the dispersed fluorescence spectrum ($\sim$12 cm^{-1}), Parmenter and co-workers were unable to identify these channels.

The intensity unaccounted for in the MATI spectrum appears to be significant. Thirty to fifty percent of the most intense vibrational predissociation band, which is a blending of the 0_0^0 and 6_1^1 ($D_0 \leftarrow S_1$) transitions, i.e., it includes both the 6^1 and 0^0 destination states, is not accounted for in Lembach and Brutschy's analysis. Their fitting procedure assumed that the rotational contours for transitions arising from 6^1 and 0^0 pDFB would be Gaussian in shape and have the same widths. However, since the excess energy available is considerably more in the case of 0^0 (451 cm^{-1}, cf. 41 cm^{-1} for 6^1), transitions from 0^0 might show considerably broader rotational contours due to increased rotational excitation of the pDFB fragments produced in this state. The 8_0^1 ($D_0 \leftarrow S_1$) band in Fig. 10 of Lembach and Brutschy's paper appears to be broader than the 6_1^0 ($D_0 \leftarrow S_1$) band, supporting this proposition. Consequently, we suggest that the estimate that 30%–50% of the intensity cannot be explained by population of 6^1 and 0^0 alone represents an upper limit.

Because of the importance of the pDFB vibrational distribution to the present study, our group has recently measured a higher resolution ($\sim$1 cm^{-1}) dispersed fluorescence spectrum from the $\overline{5^1}$ level in the region of the 6_1^1 and 0_0^0 bands. This has been undertaken as part of a wider exploration of the vibrational population distribution in pDFB fragments from pDFB–Ar dissociation that will be reported in a

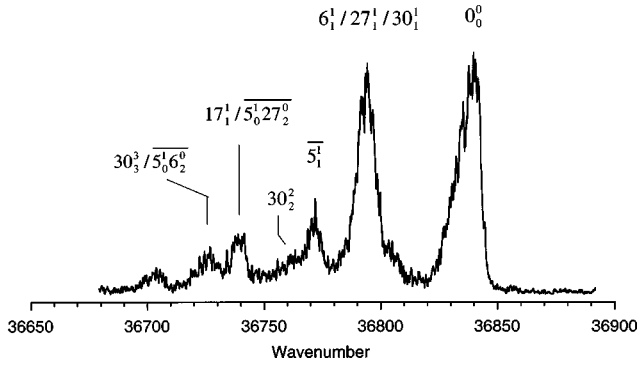

FIG. 5. A section of the dispersed fluorescence spectrum following excitation of the $\overline{5^1}$ level in pDFB–Ar. This section covers the region where the 0_0^0, 6_1^1, 17_1^1, 27_1^1, 30_1^1, 30_2^2, and 30_3^3 bands would appear (see text). The positions where each of these bands would appear is indicated.

future publication.[34] This spectrum, shown in Fig. 5, reveals that $6^1/27^1/30^1$ and 0^0 are the dominant channels, with 46% transfer to each. The remaining vibrations with observable population are 8^1 and $8^1 30^1$ (not seen in the region of the spectrum displayed in Fig. 5) each with only 4%. A very weak shoulder appears on the low-energy side of the $\overline{5_1^1}$ band and is assigned to the 30_2^2 band, showing that while transfer to 30^2 is occurring, it is minimal and can be ignored. The 17_1^1 and 30_3^3 bands overlap with the $\overline{5_0^1 27_2^0}$ and $\overline{5_0^1 6_2^0}$ transitions from $\overline{5^1}$, respectively. Comparisons between 5^1 and $\overline{5^1}$ dispersed fluorescence spectra show that any transfer to 17^1 and 30^3 is very small since the relative intensities of the $\overline{5_1^1}$ (no overlap with product states), $\overline{5_0^1 27_2^0}$, and $\overline{5_0^1 6_2^0}$ bands are not changed as they would if growth bands were present. From the dispersed fluorescence spectrum we can rule out 17^1, 30^2, and 30^3 as important channels. We are unable to resolve the 6_1^1, 27_1^1, and 30_1^1 bands as these transitions overlap[35,36] and the "6_1^1" band could therefore be a combination of 6_1^1, 27_1^1, and 30_1^1. The energies of 6^1 and 27^1 are almost the same (410 and 403 cm^{-1}, respectively) and hence for the purpose of deducing the relative partitioning into vibrational, rotational, and translational energy, it is not important to distinguish between 6^1 and 27^1. Consequently, we refer to 6^1 alone in the discussion that follows, while implicitly recognizing that 27^1 could also be a contributor.

From the energy of $\overline{5^1}$ (818 cm^{-1}) and the binding energy of the complex in S_1 (367 ± 4 cm^{-1}), the excess energies available to pDFB fragments produced in the 0^0, 30^1, and 6^1 levels are calculated to be 451, 331, and 41 cm^{-1}, respectively. The shape of the TER distribution indicates that the 30^1 contribution may be significant. From the fits to Figs. 1 and 3 and the estimate that the distribution in Fig. 1 has a 25% contribution from dissociation in D_0, the distribution for dissociation from $\overline{5^1}$ alone can be determined. The $\overline{5^1}$ TER distribution has 60% of the molecules with translational energy less than 41 cm^{-1}, i.e., 60% of the products are produced with translational energy less than the total energy available to the products when pDFB is formed in 6^1. If 6^1 and 0^0 were the only destination states populated, the TER distribution for 0^0 would have 10% below 41 cm^{-1} and 40% above. The TER distribution for populating 6^1 from $\overline{5^1}$ is likely to be similar to that for populating 0^0 from $\overline{6^1}$ since the excess energies are almost the same. (The latter distribution has been reported previously.[28]) If this is the case, population of 6^1 and 0^0 alone would lead to an odd shape for the TER distribution for 0^0, with a discontinuity around 41 cm^{-1}. Consequently, we suggest that it is likely that 30^1 is populated, however from the data at hand the fraction of population in this level cannot be determined.

Before proceeding we comment further on the shape of the TER distribution seen in Fig. 1. The distribution is smooth and featureless, showing no structure. Three vibrational levels, 0^0, 30^1, and 6^1, appear to be significantly populated. If the pDFB fragments were produced with minimal rotation, the excess energy would appear as translation and the TER distribution would consist of three bands, at 41 cm^{-1} (populating 6^1), 331 cm^{-1} (populating 30^1), and 451 cm^{-1} (populating 0^0). There is no hint of such structure; indeed, the distribution is approximately zero by 300 cm^{-1}, which is well before the 451 cm^{-1} released when populating 0^0, which accounts for almost 50% of the nascent vibrational distribution. Clearly there must be significant rotational excitation of the fragments. Even so, given the very limited number of vibrational states available, the absence of structure in the TER distribution is surprising. Note that the TER distribution from the cation dissociation alone (Fig. 3) is also smooth, so there is no evidence that structure from dissociation in S_1 is being masked by interference from "out of phase" structure arising from the $\sim\frac{1}{4}$ of dissociation occurring in D_0.

That a significant proportion of the excess energy appears as rotational energy of the fragments is consistent with broad linewidths being observed in the MATI spectra by Lembach and Brutschy.[6] The rotational contours of bands associated with dissociation in the S_1 state were $\geqslant 7$ times as broad as those for nondissociation S_1 resonances. In the dispersed fluorescence spectrum from $\overline{5^1}$, the linewidths of bands associated with dissociation also indicate that there is rotational excitation of the pDFB fragments.[34]

A conservative estimate of the average rotational energy released in the case of the 0^0 pDFB product can be obtained as follows. First, the one quarter contribution to the $\overline{5^1}$ TER distribution from dissociation occurring in D_0 is subtracted by assuming the D_0 TER distribution to be the same as that obtained in the $1+1'$ REMPI experiment (see Fig. 3). (Since the $\overline{5_0^1}$ and $1+1'$ REMPI TER distributions are very similar, in practice this makes very little difference to the average energy obtained.) Second, it is assumed that 30^1 is not significantly populated. (If fragments are produced in 30^1 rather than 6^1, there will be an increase in the fraction of pDFB fragments with higher excess energy and the average rotational energy will be larger than the value deduced here.) 0^0 and 6^1 are assumed to be the only levels populated and they are assumed to be populated in equal proportion. Third, the TER distribution for populating 6^1 from $\overline{5^1}$ is subtracted from the resulting distribution assuming 50% dissociation into 6^1. The TER distribution for populating 6^1 from $\overline{5^1}$ is assumed to be the same as that for populating 0^0 from $\overline{6^1}$, since the available energy is the same in both cases. This

distribution has been reported previously.[28] The average translational energy is determined from the resulting 0^0 distribution to be $E_{\text{trans}}^{\text{av}}=70\ \text{cm}^{-1}$. (Ignoring 30^1 minimizes the average excess energy and hence minimizes the rotational energy available to the pDFB fragment. If 6^1 is ignored and the final states assumed to be only 30^1 and 0^0, the average rotational energy available to 0^0 increases by 10 cm^{-1}.) For energy to be conserved, the 451 cm^{-1} of energy available must be taken up by translation and rotation. Therefore, on average ~380 cm^{-1} must be partitioned into rotational energy, i.e., $E_{\text{rot}}^{\text{av}}=380\ \text{cm}^{-1}$.

The average angular momentum of the pDFB fragment can be estimated from $E_{\text{rot}}^{\text{av}}$. Although pDFB is an asymmetric rotor, the *B* and *C* rotational constants, 0.0479 and 0.0364 cm^{-1} respectively, are comparable and significantly less than the *A* rotational constant, 0.1762 cm^{-1}.[37] pDFB is therefore a near prolate rotor. For simplicity we consider pDFB to be a prolate symmetric rotor and average the *B* and *C* rotational constants. The energy levels for a prolate symmetric rotor are given by:

$$E(J,K)=CJ(J+1)+(A-C)K^2. \tag{2}$$

From this expression we can determine approximate maximum and minimum values for the angular momentum quantum number, *J*, corresponding to an average rotational energy of 380 cm^{-1}. J_{max} occurs when $K=0$ and J_{min} when $K=J$. When *J* is large and $K=0$, Eq. (2) reduces to

$$E(J_{\text{max}},0)\approx C(J_{\text{max}})^2=380\ \text{cm}^{-1}$$

and $J_{\text{max}}=95$. Similarly, when *J* is large and $K\approx J$

$$E(J_{\text{min}},K=J)\approx C(J_{\text{min}})^2+(A-C)(J_{\text{min}})^2 = 380\ \text{cm}^{-1},$$

and $J_{\text{min}}=46$.

Maximum and minimum values for the rotational angular momentum ($\sqrt{J(J+1)}\hbar\approx J\hbar$) are therefore 1.0×10^{-32} and 4.8×10^{-33} Js, respectively. For angular momentum to be conserved the rotational angular momentum must equal the orbital angular momentum. The orbital angular momentum, *L*, is related to the impact parameter, *b*, by

$$L=\mu v b. \tag{3}$$

Here μ is the reduced mass of pDFB–Ar and v is the velocity of the fragments. The average velocity can be estimated from the average kinetic energy released to the fragments, $E_{\text{trans}}^{\text{av}}$. From Eq. (3) we determine that impact parameters corresponding to the average rotational energy will be in the range 1.8–3.7 Å. This range for *b* gives an indication of the distance of the center of the Ar atom from the center of the pDFB ring at the transition state. For comparison, the C–C bond length is ~1.4 Å. A distance of 1.8 Å places the center of the Ar atom beyond the centers of the C atoms. In order for high rotational energy to occur in the pDFB molecule, the Ar atom must be largely off-center from the pDFB molecule when the complex dissociates. Hence a large value of *b* is required.

The analysis above reveals that the majority of the excess energy is in the pDFB product rotation when 0^0 is the product vibrational level. In this case the available energy is 451 cm^{-1}. Is there significant rotational excitation of the product if there is less energy available to translation and rotation? As we have noted earlier, the observation of smooth TER distributions suggests that this is so. Other data support this. We have previously reported the TER distributions for dissociation from $\overline{6^1}$ and $\overline{6^1 s^1}$, where *s* denotes the van der Waals stretch.[28] In both cases the excess energy is small (41 and 83 cm^{-1} for $\overline{6^1}$ and $\overline{6^1 s^1}$, respectively) and the only destination level available is 0^0. Thus the excess energy can only appear in translation and rotation. The TER distributions both peak at low energy (below 20 cm^{-1}), revealing that the products are rotationally excited. Lembach and Brutschy observed a broad linewidth to bands originating from the 6^1 product in dissociation from $\overline{5^1}$ where the total excess energy is only 39 cm^{-1}.[6] The evidence is that significant rotational excitation of the pDFB fragment occurs for all destination levels, not just those involving a large excess energy.

The mechanism of dissociation is for IVR to first redistribute energy to the van der Waals modes.[1] In a previous publication we pointed out that, once sufficient energy has been transferred from the pDFB vibrational modes to the van der Waals modes, the Ar atom is above the barrier to switching from one side of the ring to another and is able to move around the pDFB chromophore.[29] Calculations for benzene–Ar suggest that this barrier is ~200 cm^{-1},[38] which is well below the S_1 dissociation energy of 369 cm^{-1}.[28,29] The large value of *b* we obtain is consistent with the proposition that the geometry of the pDFB–Ar complex is not constrained near equilibrium prior to dissociation, as has been suggested previously in regard to dissociation of van der Waals complexes.[8]

B. Dissociation of pDFB–Ar^+ from $\underline{29_2}$

Unlike the case for $\overline{5^1}$, there are no data available concerning the distribution of population amongst the vibrational levels of $pDFB^+$ following dissociation of pDFB–Ar^+ from $\underline{29_2}$. However, the evidence strongly suggests that 0_0 will be the dominant destination level. First, the higher dissociation energy for the complex[28,29] means that only 445 cm^{-1} of energy are available, giving only ten possible destination levels.[31] Second, Parmenter and co-workers observed in their studies of dissociation within S_1 that only a few of the vibrational modes were populated and that these were largely the same for all the initial states excited.[2–4] On this basis very few of the ten possible destination levels will be accessed. Third, the vibrational frequencies are similar in D_0 and S_1.[31] Consequently it is likely that the dissociation process from $\underline{29_2}$ favors the same destination levels as seen from $\overline{29^2}$ in S_1, with the caveat that some vibrations may be inaccessible in D_0 because of the increased dissociation energy. Dissociation from $\overline{29^2}$ populates 6^1 (53%), 29^1 (36%), and 0^0 (11%).[2–4] 29_1 is inaccessible from $\underline{29_2}$ and population of 6_1 will release only 5 cm^{-1} of excess energy. Consequently, of the analogous levels to those accessed from $\overline{29^2}$, only 0_0 will lead to a TER distribution above 5 cm^{-1}. (A caveat here is that, because of the inability to distinguish 6^1

and 30^1 in the dispersed fluorescence studies of dissociation from $\overline{29^2}$, there could be a contribution from 30_1, but the excess energy available in that case is also large and so the qualitative conclusions determined for 0_0 also apply to 30_1.) In the following we examine the consequences that follow if 0_0 is the dominant destination level below 6_1.

Dissociation to 0_0 releases 444 cm^{-1}. Since the translational energy distribution peaks below 100 cm^{-1} and is zero by ~300 cm^{-1}, there must be significant rotational excitation of the $pDFB^+$ fragment. The average translational energy is 60 cm^{-1}, giving an average rotational energy in 0_0 of ~384 cm^{-1}. This is essentially the same value determined for 0^0 in dissociation from $\overline{5^1}$, and so is not unreasonable.

If 0_0 is the dominant destination level below 6_1, the impact factor will be similar to that deduced for 0^0 produced from $\overline{5^1}$ dissociation since the average rotational energies are similar in the two cases. Assuming 0_0 to the dominant destination level below 6_1 is the extreme that yields the largest rotational excitation. Nevertheless, since the TER distribution has decayed to essentially zero ~150 cm^{-1} less than the excess energy available for the 0_0 product, if 0^0 is populated to any significant extent (and the evidence points to this being the most likely outcome), the 0_0 $pDFB^+$ product must be excited rotationally.

V. CONCLUSIONS

Translational energy release (TER) distributions have been presented following excitation of the $\overline{5_0^1}$ and $\overline{29_0^2}$ transitions in pDFB–Ar. Evidence has been presented showing that these TER distributions correspond primarily to dissociation from $\overline{5^1}$ in S_1 pDFB–Ar and $\overline{29_2}$ in D_0 pDFB–Ar^+. Analysis of the TER distributions in combination with the vibrational distributions of the pDFB/$pDFB^+$ product leads to the following conclusions:

(1) Surprisingly, no structure is seen in any of the TER distributions reported even though there are only a few, widely spaced vibrational levels that can be accessed. The absence of structure points to the products having significant rotational excitation so that the distribution is ''filled in.''

(2) Rotational motion appears to be an important reservoir for the excess energy. In the case of dissociation from $\overline{5^1}$, the average rotational energy in the 0^0 level of the pDFB product is 5.4 times the average translational energy released. For $\overline{29_2}$ the situation is less well defined due to the absence of data for the vibrational levels populated in the $pDFB^+$ product. Nevertheless, assuming the vibrational propensities for $\overline{29_2}$ to be similar to those seen for the $\overline{29^2}$ level in S_1 pDFB–Ar, we find that similar ratios of rotational to translational energy are likely for $\overline{29_2}$ and $\overline{5^1}$. Qualitatively we find that in every case where there are data concerning the pDFB product it is rotationally excited, even when only modest amounts of energy are released.

(3) The high rotational excitation observed in the 0^0 pDFB product following dissociation from $\overline{5^1}$ suggests impact parameters greater than the C–C bond length, placing the Ar beyond the aromatic ring at the point of dissociation. The complex does not appear to dissociate from a well-constrained geometry close to the equilibrium configuration (which has the Ar above the center of the aromatic ring) as has been suggested previously as a reason for differences between van der Waals predissociation and collision-induced vibrational energy transfer.[8]

We noted in the Introduction that a number of previous experiments have revealed rotational excitation of fragments in van der Waals complex dissociation.[5–6,9–12] It appears that significant rotational excitation of fragments is common in van der Waals molecule dissociation, at least in the sparse regions of the vibrational manifold of the products. The extent to which rotation remains an important energy reservoir at higher levels of vibrational state density (and hence higher density in the vibrational manifold of the products) is an interesting question for future research.

ACKNOWLEDGMENTS

This work was undertaken with the financial support of the Australian Research Council and Flinders University. The authors are grateful for the technical support provided by the staff of the School of Chemistry, Physics and Earth Sciences Engineering and Electronic Workshops. We thank Rebecca Moulds for providing us with the $\overline{5^1}$ pDFB–Ar dispersed fluorescence spectrum and its analysis. Special thanks go to Dr. Jason Gascooke who designed the apparatus, wrote the software, and made it all work. S.M.B. acknowledges scholarship support from the Australian Government.

[1] E. R. Bernstein, Annu. Rev. Phys. Chem. **46**, 197 (1995).
[2] K. W. Butz, D. L. Catlett, Jr., G. E. Ewing, D. Krajnovich, and C. S. Parmenter, J. Phys. Chem. **90**, 3533 (1986).
[3] H.-K. O, C. S. Parmenter, and M.-C. Su, Ber. Bunsenges. Phys. Chem. **92**, 253 (1988).
[4] B. D. Gilbert, C. S. Parmenter, and H.-K. O, J. Phys. Chem. **99**, 2444 (1995).
[5] G. Lembach and B. Brutschy, J. Phys. Chem. **100**, 19758 (1996).
[6] G. Lembach and B. Brutschy, J. Phys. Chem. A **102**, 6068 (1998).
[7] S. A. Rice, J. Phys. Chem. **90**, 3063 (1986).
[8] V. Bernshtein and I. Oref, Chem. Phys. Lett. **300**, 104 (1999).
[9] D. V. Brumbaugh, J. E. Kenny, and D. H. Levy, J. Chem. Phys. **78**, 3415 (1983).
[10] X. Zang, J. M. Smith, and J. L. Knee, J. Chem. Phys. **97**, 2843 (1992).
[11] H. Saigusa, B. E. Forch, K. T. Chen, and E. C. Lim, Chem. Phys. Lett. **101**, 6 (1983).
[12] M. A. Hoffbauer, K. Liu, C. F. Giese, and W. R. Gentry, J. Chem. Phys. **78**, 5567 (1983).
[13] M. F. Vernon, J. M. Lisy, H. S. Kwok, D. J. Krajnovich, A. Tramer, Y. R. Shen, and Y. T. Lee, J. Phys. Chem. **85**, 3327 (1981).
[14] I. Nishiyama and I. Hanazaki, Chem. Phys. Lett. **117**, 99 (1985).
[15] R. D. Johnson, S. Burdenski, M. A. Hoffbauer, C. F. Giese, and W. R. Gentry, J. Chem. Phys. **84**, 2624 (1986).
[16] K. Ohashi and N. Nishi, J. Chem. Phys. **98**, 390 (1993).
[17] L. M. Yoder and J. R. Barker, Phys. Chem. Chem. Phys. **2**, 813 (2000).
[18] L. M. Yoder, J. R. Barker, K. T. Lorenz, and D. W. Chandler, Chem. Phys. Lett. **302**, 602 (1999).
[19] J. R. Gascooke and W. D. Lawrance, J. Phys. Chem. A **104**, 10328 (2000).
[20] A. T. J. B. Eppink and D. H. Parker, Rev. Sci. Instrum. **68**, 3477 (1997).
[21] D. W. Chandler and P. L. Houston, J. Chem. Phys. **87**, 1445 (1987).
[22] M.-C. Su, H.-K. O, and C. S. Parmenter, Chem. Phys. **156**, 261 (1991).
[23] B. A. Jacobson, S. Humphrey, and S. A. Rice, J. Chem. Phys. **89**, 5624 (1988).

[24] R. Sussmann, R. Neuhauser, and H. J. Neusser, Can. J. Phys. **72**, 1179 (1994).
[25] R. Sussmann and H. J. Neusser, J. Chem. Phys. **102**, 3055 (1995).
[26] P. Hobza, H. L. Selzle, and E. W. Schlag, J. Chem. Phys. **99**, 2809 (1993).
[27] P. Tarakeshwar, K. Kim, E. Kraka, and D. Cremer, J. Chem. Phys. **115**, 6018 (2001).
[28] S. M. Bellm, J. R. Gascooke, and W. D. Lawrance, Chem. Phys. Lett. **330**, 103 (2000).
[29] S. M. Bellm, R. J. Moulds, and W. D. Lawrance, J. Chem. Phys. **115**, 10709 (2001).
[30] G. Reiser, D. Rieger, T. G. Wright, K. Müller-Dethlefs, and E. W. Schlag, J. Phys. Chem. **97**, 4335 (1993).
[31] E. W. Hanson and P.-L. Law, J. Opt. Soc. Am. A **2**, 510 (1985).
[32] E. Sekreta, K. S. Viswanathan, and J. P. Reilly, J. Chem. Phys. **90**, 5349 (1989).
[33] S. W. Allendorf, D. J. Leahy, D. C. Jacobs, and R. N. Zare, J. Chem. Phys. **91**, 2216 (1989).
[34] R. J. Moulds and W. D. Lawrance (unpublished results).
[35] R. A. Coveleskie and C. S. Parmenter, J. Mol. Spectrosc. **86**, 86 (1981).
[36] A. E. W. Knight and S. H. Kable, J. Chem. Phys. **89**, 7139 (1988).
[37] T. Cvitas and J. M. Hollas, Mol. Phys. **18**, 793 (1970).
[38] B. Fernandez, H. Koch, and J. Makarewicz, J. Chem. Phys. **111**, 5922 (1999).